Comparative study of the prediction of delayed strains using the next-generation Eurocode2 with measurements on structures

Francis Barré, Ludovic Caba, Jean Michel Torrenti, Abudushalamu Aili

Comparative study of the prediction of delayed strains using the next-generation Eurocode2 with measurements on structures

Francis Barré[1*], Ludovic Caba[2], Jean Michel Torrenti[3,4], Abudushalamu Aili[5]

[1]Géodynamique et Structure, [2] EDF DIPNN DT, [3] Université Gustave Eiffel, [4] ESITC Paris, [5] Nagoya University

[*] Corresponding Author, E-mail: jean-michel.torrenti@univ-eiffel.fr

Abstract: In structures where prestressing plays a vital role, predicting stress losses is essential to demonstrate their robustness. After presenting the equations of the next-generation Eurocode 2 (EC2), the delayed deformations of the containment vessels of EDF nuclear power plants are predicted. In the first step, the parameters of the laws are recalibrated based on the measurements of the containments, considering a temperature higher than 20°C. The application to 17 containments allows for the definition of a safety coefficient to be applied to shrinkage and creep to ensure that the delayed deformations evaluated for the design will be conservative. In the second step, the parameters of the equations of creep and shrinkage are calibrated on laboratory results, and an analytical model using these parameters is applied to 5 containments. All the results show that it is possible to predict the behavior of prestressed structures provided that the parameters of the equations controlling the delayed deformations are calibrated either on measurements of these structures or laboratory tests. Considering the variability of concretes, safety coefficients are proposed to guarantee that the predicted deformations cover 95% of the deformations of concrete of a given strength.

KEYWORDS: Concrete, Prestress, Shrinkage, Creep, EC2, fib model code, Monitoring

1. Introduction

In all structures where prestressing plays a vital role, predicting prestress force losses is essential for demonstrating their robustness. When the post-tensioned tendons are protected by grouting, it is impossible to compensate for the losses by a supplementary tension. In the case of long-span bridges, a prestressing loss could induce large deflections (Bazant et al., 2011; Bazant, 2012a; Bazant, 2012b; Aili et al., 2023). In nuclear containments, prestressing is needed to guarantee safety or increase the service life (Abrishami et al., 2015). This prediction can be made using constitutive relations for shrinkage, concrete creep, and reinforcement relaxation. For instance, the B4 model has been used for bridges (Wendner et al., 2015), and several models were used by several authors for nuclear reactor containments (Lundqvist & Nilsson, 2011; Song et al., 2007; Hora & Patzak, 2007). Here, the relation proposed in the next generation Eurocode 2 (ngEC2) is used to predict the delayed behavior of several French nuclear power plants (NPPs) containments.

The ngEC2, which is currently being finalized (CEN, 2022), has introduced new relationships for concrete shrinkage and creep laws based on the fib Model Code 2010 – MC2010 (fib, 2012) (Muller et al., 2013). It also confirmed the possibility, as it is already the case for the current EN1992-2 (EC2) - bridges section (AFNOR, 2005), to calibrate the parameters of the relationships either on measurements on structures or laboratory tests.

After presenting the shrinkage and creep constitutive relations of the ngEC2, these relations are applied to predict delayed deformations of EDF's nuclear containments (including the Vercors mock-up), for which special monitoring attention has been carried out, and measurements over many years are available. Two strategies are tested.

Initially, as allowed by the ngEC2, the parameters of the relations to predict creep and shrinkage are recalibrated with the containment monitoring measurements on 17 prestressed concrete containments, taking into account a temperature greater than 20°C, with the laws proposed by the model code *fib* 2010.

In the second approach, the parameters are calibrated with laboratory concrete specimen results, and analytical modelling using these parameters is applied for a containment mock-up and 4 containments.

Finally, the results will be analyzed to determine a safety factor to be applied to shrinkage and creep to ensure that the delayed deformations evaluated for the design will be conservative.

2. Constitutive relations

2.1 Shrinkage and creep in the next-generation EC2

In modern concrete codes such as the ngEC2, which will be used after, the delayed deformation of concrete ε^c is separated into 4 parts:

$$\varepsilon^c = \varepsilon^{bs} + \varepsilon^{ds} + \varepsilon^{bc} + \varepsilon^{dc} \quad (1)$$

where ε^{bs} is the autogenous shrinkage, ε^{ds} is the drying shrinkage, ε^{bc} is the basic creep, and ε^{dc} is the drying creep. Autogenous shrinkage and drying shrinkage are functions of the compressive strength of concrete f_{cm} and the drying time t - t_s:

$$\varepsilon^{bs} = \xi_{cbs1}\alpha_{bs}\left(\frac{0,1\,f_{cm}}{6+0,1\,f_{cm}}\right)\left(1 - e^{-0,2\xi_{cbs2}\sqrt{t}}\right) \quad (2)$$

$$\varepsilon^{ds} = \xi_{cds1}[(220 + 110\alpha_{ds1})e^{-\alpha_{ds2}f_{cm}}]\beta_{RH}\left[\frac{(t-t_s)}{0,035\xi_{cds2}h^2+(t-t_s)}\right]^{0,5} \quad (3)$$

$\varepsilon^{ds} = \xi_{cds1}\left[(220 + 110\alpha_{ds1})e^{-\alpha_{ds2}f_{cm}}\right]\beta_{RH}\left[\frac{(t-t_s)}{0,035\xi_{cds2}h^2+(t-t_s)}\right]^{0,5}$ where α_{bs}, α_{ds1}, and α_{ds2} are parameters that depend on the type of cement; h is the notional size of the concrete element; t_s is the age from which concrete begins to dry; ξ_{cbs1}, ξ_{cds1}, ξ_{cbs2}, and ξ_{cds2} are parameters to be adjusted either on laboratory tests or on measurements of the structure concerned (the default values being equal to 1). β_{RH} is a function that depends on RH relative humidity.

For basic creep and desiccation creep, the evolution is given by the creep coefficients, i.e., $\varepsilon^{bc}(t,t0) = \sigma_0\,\varphi_{bc}(t,t_0)/E_c$ and $\varepsilon^{dc}(t,t0) = \sigma_0\,\varphi_{dc}(t,t_0)/E_c$ where σ_0 is the applied stress, t_0 is the age of the concrete at the time of loading, and E_c is the concrete Young's modulus. For basic creep, the creep coefficient is written as:

$$\varphi_{bc}(t,t_0) = \xi_{bc1}\frac{1,8}{(f_{cm})^{0,7}}ln\left(1 + \left(\frac{30}{t_{0,adj}} + 0,035\right)^2\frac{(t-t_0)}{\xi_{bc2}}\right) \quad (4)$$

where $t_{0.adj}$ is the loading age adjusted to account for the type of cement and the curing temperature; ξ_{bc1} and ξ_{bc2} are parameters that can be adjusted based on experimental results (the default values are equal to 1).

For desiccation creep, the creep coefficient is written as:

$$\varphi_{dc}(t,t_0) = \xi_{dc1}\beta_{dc}(f_{cm},RH,t_0)\left[\frac{t-t_0}{\xi_{dc2}\beta_h+t-t_0}\right]^{\gamma(t_0)} \quad (5)$$

With:

$$\beta_{dc}(f_{cm},RH,t_0) = \frac{412}{(f_{cm})^{1.4}}\frac{1-\frac{RH}{100}}{\sqrt[3]{0.1\frac{h}{100}}}\frac{1}{0.1+(t_{0,adj})^{0.2}} \quad (6)$$

$$\gamma(t_0) = \frac{1}{2,3+3,5/\sqrt{t_{0,adj}}} \quad (7)$$

$$\beta_h = min\left\{1,5h + 250\left(\frac{35}{f_{cm}}\right)^{0,5};\ 1500\left(\frac{35}{f_{cm}}\right)^{0,5}\right\} \quad (8)$$

ξ_{dc1} and ξ_{dc2} are parameters that can be adjusted based on experimental results (default values are 1).

Because, from the material point of view, these relations mainly depend on the mean compressive

strength f_{cm}, a large variability is observed between the strains predicted using these equations and the real ones (Shurbert-Hetzel et al., 2023; Smilauer, 2023). In MC2010, coefficients of variation equal to 25% for creep and 35% for shrinkage are indicated. In ngEC2, a coefficient of variation equal to 30% is shown as usual. And the ξ_i coefficients are included in these equations to match the observed deformations.

2.2 Effect of the temperature on the constitutive relations

In operation, the ambient temperature inside the containment increases, and the average cylinder wall temperature exceeds 20 °C. It affects the delayed strains of the containment vessel (Anderson, 2005), (Bouhjiti et al., 2018). The relations presented are adapted to consider the temperature. The monitoring of seventeen containments since the prestressing is used to recalibrate the laws. This monitoring includes temperature, relative humidity and strains measurements.

The adaptations to account for temperature are derived from the laws described in the 2010 *fib* Model Code (*fib*, 2012). Temperature is not considered for the evaluation of autogenous shrinkage because this deformation mainly occurs before the reactor operation starts. The kinetics of desiccation shrinkage are accelerated by multiplying $0{,}035\xi_{cds2}h^2$ by the factor $\exp[-0{,}06(T-20)]$. The maximum amplitude of drying shrinkage is increased by the factor $\beta_{st} = 1 + [4/(103 - RH)]\,[(T-20)/40]$.

The basic creep and desiccation creep coefficients are multiplied by the factor $\varphi_T = exp[0{,}015\,(T-20)]$:

$$\varphi_{bc,T}(t,t_0) = \varphi_{bc}(t,t_0)\varphi_T \quad (9)$$

$$\varphi_{dc,T}(t,t_0) = \varphi_{dc}(t,t_0)\,\varphi_T^{1,2} \quad (10)$$

Finally, the kinetics of desiccation creep are accelerated by the factor $\beta_{HT} = \beta_H\ \beta_T$, where β_H corresponds to the influence of the relative humidity and β_T to the influence of temperature. β_T is given by the following equation:

$$\beta_T = exp\left[\frac{1500}{273+T} - 5{,}12\right] \quad (11)$$

3. Recalibration of the constitutive relations with containment measurements

In France, the prestressed concrete containment of all reactor buildings is equipped with monitoring devices such as extensometers and thermocouples (Simon & Courtois, 2011). The monitoring sensors acquired data since the beginning of the construction, before the post-tensioning, and are still used nowadays.

At the end of the construction, the containment is tensioned by prestress tendons. For containment walls, which are compressed in the tangential and vertical directions, the creep formulae are adapted by replacing σ_0/E_c by the initial deformation in the direction considered for the basic creep and by $(\sigma_T + \sigma_V)/E_c$ for the desiccation creep, with σ_T the applied stress in the tangential direction and σ_V in the vertical direction (see figure 1). These initial deformations $(\sigma_T - \nu.\,\sigma_V)/E_c$ and $(\sigma_T + \sigma_V)/E_c$ are calculated values with the design data (compressive strength) and the Young's modulus and Poisson's ratio measured during the pressure test.

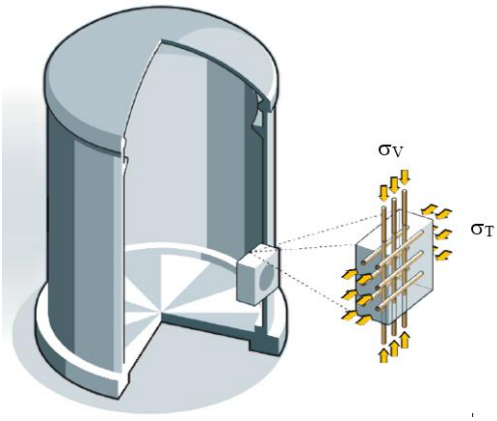

Figure 1 – Prestressing stresses applied

This methodology aligns with the the measurements on the containments and the French national annex of EN1992-1-1 (AFNOR, 2007). According to this text, the creep is to be considered an anisotropic deformation proportional to the instantaneous deformation in the direction considered, and the creep of desiccation is to be considered to produce isotropic strains.

Before the nuclear power plant is commissioned, the containment is subjected to a pressure test to assess both leak-tightness and strength. The initial deformations were calculated from the values of Young's modulus E_c and the Poisson coefficient ν of the wall of each unit, as determined during the test of the containment's resistance to internal pressure (see Figure 2).

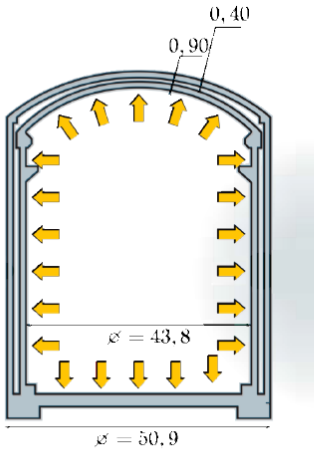

Figure 2 – Containment under the effect of pressure test (an inner pressure is applied in the containment depending on the standard)

Seventeen varied containment buildings of NPP in operation are included in the analysis. Four of them correspond to single-lined 900 mm-wall. The remaining thirteen containments correspond to a double containment wall design without metallic liner. They are representative of three typical standard geometries, with a thickness equal to:

- 900 mm for the standard P4,
- 1200 m for the standard P'4 and N4.

The figure 3 illustrates the difference between the 4 single 900 MWe containments and the 13 1300 MWe double containments.

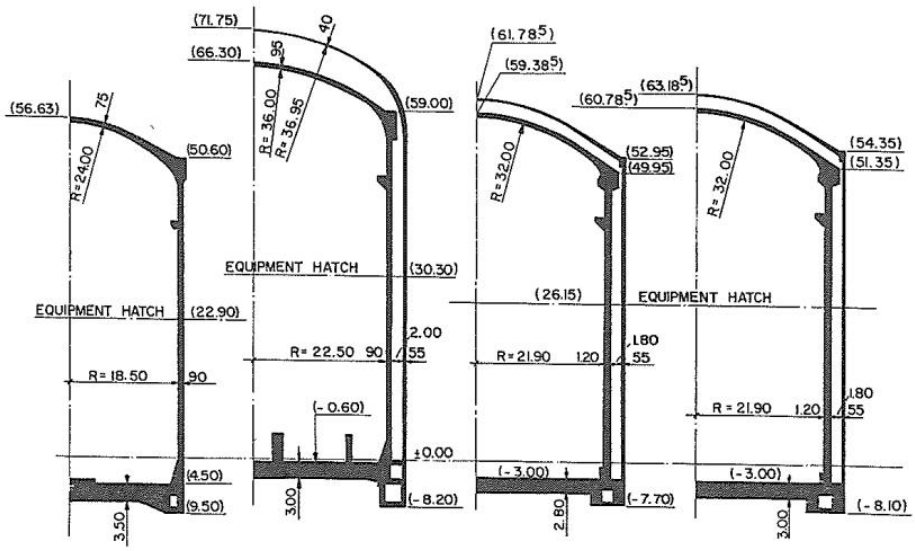

Figure 3: **Single containment with metallic liner and 3 standard geometries of double containment without liner (extract from JL Costaz 83 - Figure courtesy of IASMiRT)**

Figure 4 shows, for a single containment with liner, the temperature evolution measures in the containment wall (average value of 2 or 4 thermocouples embedded in the wall) and the comparison of the tangential and vertical strains obtained from the monitoring sensors and the theoretical values derived from ngEC2 expressions before calibration.

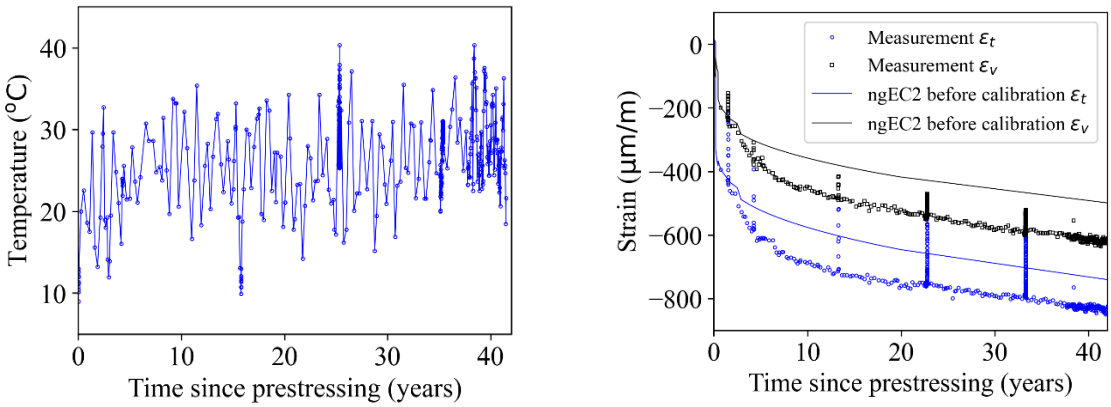

Figure 4: **Example of temperature measured, measured strains, and theoretical values before recalibration for a single containment with a liner**

Figure 5 shows the same observations for a double containment without liner: temperature evolution measures and a comparison between the tangential and vertical measured deformations and theoretical values before calibration.

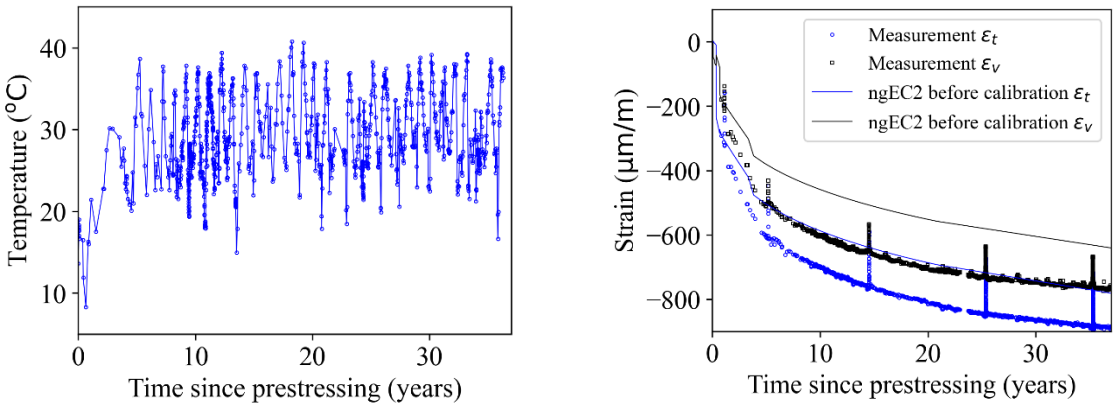

Figure 5: **Example of temperature measured, of measured strains, and of theoretical values before recalibration for a double containment without liner**

These single containments with liner are calculated with a temperature of 27.5 °C, an environmental humidity RH = 50%, and a notional size h for drying of 1800 mm to consider the watertight internal face (because the equivalent drying distance is approximated as being twice the thickness of the wall). The double wall containments without liner are calculated with a temperature of 35 °C, a RH relative humidity = 20 %, and a notional size h for drying equal to the wall thickness equal: 900 mm or 1200 mm according to the standard geometry.

The objective of the calibration procedure from measurements on containments is to determine the correction coefficients ξ_{cds1}, ξ_{cds2}, ξ_{bc1}, ξ_{bc2}, ξ_{dc1}, and ξ_{dc2} to apply to theoretical formulas (obtained with equations 1 to 11 and correction coefficients equal to 1) to coincide with the measured values. The measurements, which begin shortly before prestressing long term after concreting, do not allow the determination of correction coefficients for autogenous shrinkage.

With the hypothesis of the French annex, instantaneous strains and basic creep are proportional to the applied stresses (with a Poisson effect) while drying creep is proportional to the mean stress. With these assumptions, the tangential and vertical deformations during the time are:

$$\varepsilon_T = \left(\frac{\sigma_T - \nu\sigma_V}{E_{cm}}\right) \cdot (1 + \varphi) + \varepsilon_{isotrope} \qquad (12)$$

$$\varepsilon_V = \left(\frac{\sigma_V - \nu\sigma_T}{E_{cm}}\right) \cdot (1 + \varphi) + \varepsilon_{isotrope} \qquad (13)$$

The coefficients E_{cm} and ν are the Young modulus and the Poisson ratio determined from the behaviour od the containment during pressure tests, φ is relative to basic creep strains, and $\varepsilon_{isotrope}$ is the summation of drying creep and shrinkage deformations.

The principle is to consider the difference between tangential and vertical measured deformations that characterize the basic creep. The coefficient φ factor is determined by the 2 coefficients ξ_{bc1} and ξ_{bc2}.

Then, the average of the tangential and vertical measured deformations that characterize drying creep and shrinkage allows us to determine the four coefficients ξ_{cds1}, ξ_{cds2}, ξ_{dc1}, and ξ_{dc2}. The solution for desiccation is, therefore, not unique.

Table 1 gives the values of these coefficients for a single containment and a double containment calibrated on the measurements presented in Figures 4 and 5.

Table 1: **Example of calibration coefficients to follow the measurements**

	ξ_{cds1}	ξ_{cds2}	ξ_{bc1}	ξ_{bc2}	ξ_{dc1}	ξ_{dc2}
Single containment	1,1	0,3	1	1	1,1	0,3

Double containment	1,25	0,4	0,8	0,9	1,25	0,4

Figures 6 and 7 compare the tangential and vertical deformations measured with the theoretical values calibrated according to Table 1.

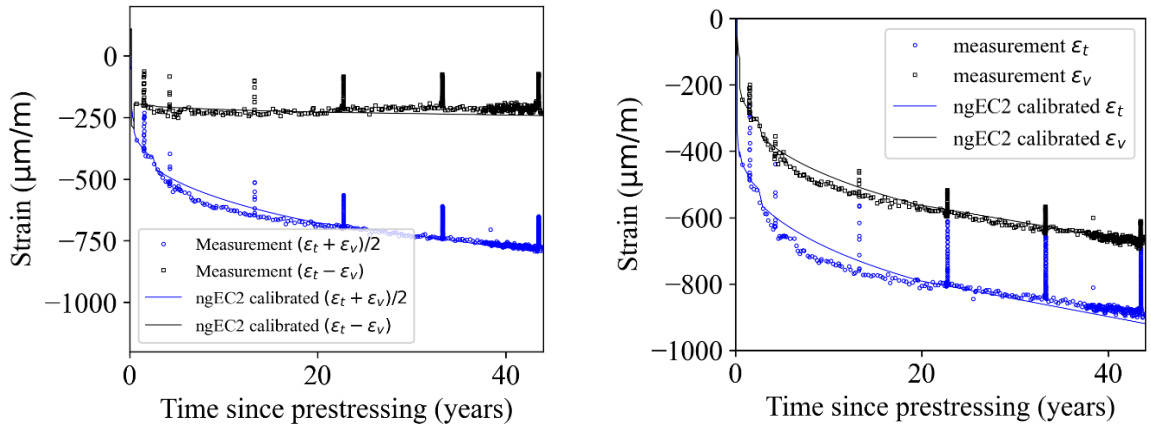

Figure 6: Example of measured strains and recalibrated theoretical values: difference average values between tangential and vertical strains, and tangential strains and vertical strains for a single containment

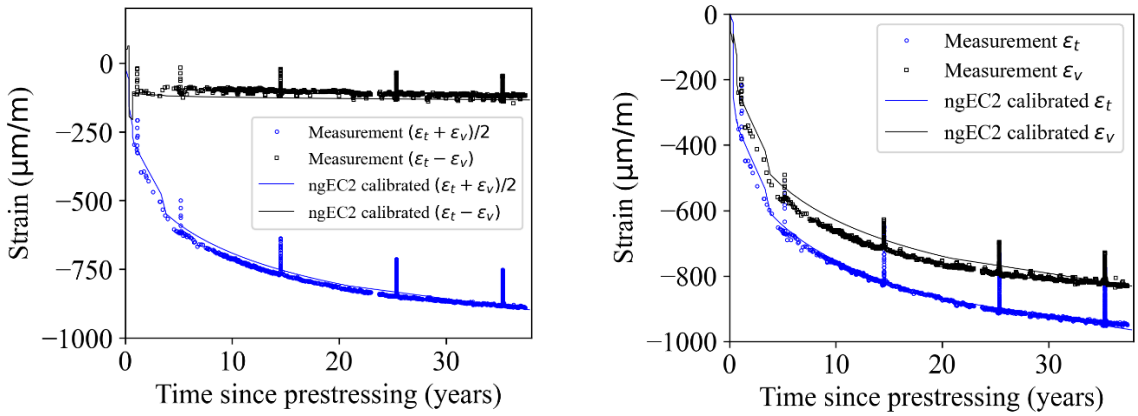

Figure 7: **Example of measured strains and recalibrated theoretical values: difference average values between tangential and vertical strains, and tangential strains and vertical strains for a double containment**

The same procedure is carried out for measurements on the seventeen containments. The ratios between the measurements (in fact, the theoretical value with correction coefficient) and the theoretical value are determined for shrinkage and creep in the long term (about 40 years). The ratio for shrinkage gives the difference for each containment between the theoretical value and the measured value according to the ngEC2. The average value between the tangential and vertical prestressing losses shall be used for the mean creep coefficient, which includes basic creep and desiccation creep. For each containment, the ratio for the average creep losses gives the difference between the theoretical value and the measured value according to the ngEC2. The mean value and coefficient of variation for the seventeen containments are determined for shrinkage and creep from these ratios determined for each containment.

Figure 8 shows the histograms for the shrinkage, the Gaussian curve in purple corresponding to the mean value and standard deviation determined for the 17 containments and the Gaussian curve in green corresponding to an average equal to 1 and the coefficient of variation defined by the fib Model Code

2010 for shrinkage, i.e., 35%. Figure 9 shows the histograms for creep, the Gaussian curve in purple corresponding to the mean value and standard deviation determined for the 17 containments and the Gaussian curve in blue corresponding to an average equal to 1 and the coefficient of variation defined by the *fib* Model Code 2010 for creep, i.e., 25%.

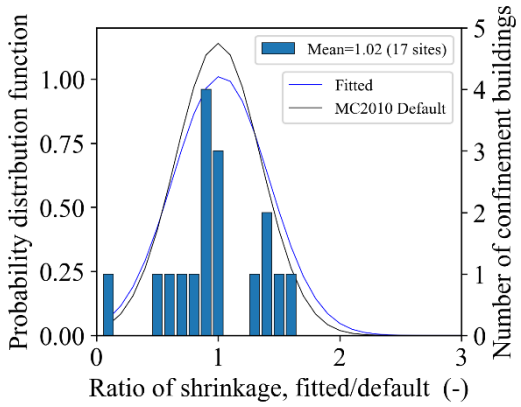

Figure 8: Histograms for shrinkage – Ratio between the theoretical values with corrective factor and theoretical values without corrective factor

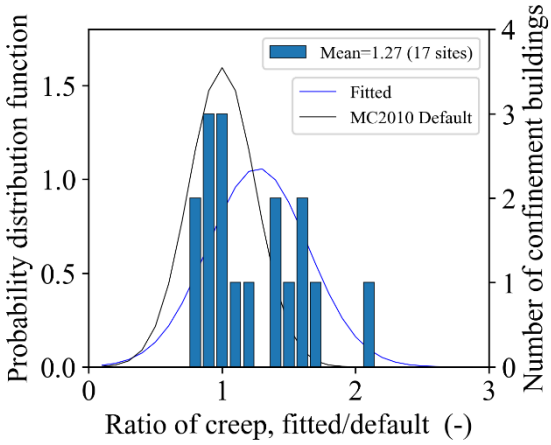

Figure 9: **Histograms for creep – Ratio between the theoretical values with corrective factor and theoretical values without corrective factor**

The figures above show a good correlation for shrinkage with a somewhat more substantial standard deviation and an underestimation for creep with a higher standard deviation.

4. Recalibration of the laws with laboratory concrete specimens

Shrinkage and creep measurements are available for the four containments noted, C1, C2, F1, and F2, and for the Vercors mock-up (Charpin et al., 2021). They are carried out under laboratory conditions (T = 20 ° C and RH = 50%) on specimens 16 cm in diameter and 1 m high (Granger, 95). Therefore, it is possible to calibrate the parameters of shrinkage and creep laws (equations 2 to 5) on these tests. Table 2 shows these adjustments.

Table 2: Adjusted parameters

	ξ_{cbs1}	ξ_{cbs2}	ξ_{cds1}	ξ_{cds2}	ξ_{bc1}	ξ_{bc2}	ξ_{dc1}	ξ_{dc2}
C1	1	1	0,9	1,3	5	5	1,5	0,4
C2	0,3	0,7	0,9	1,8	1,7	1,7	5,3	1,6
F1 & F2	0,5	0,5	1	0,4	2,6	10	1,3	0,2
Vercors	1,5	0,25	1	1,4	2,1	1,4	1,1	0,4

These laws, adjusted, are then applied in the current area of the containment (far from singularities), taking into account the multiaxial nature of the prestress (with a Poisson coefficient equal to 0.2 for basic creep) and taking into account the relaxation of the reinforcements (for the detail of the approach see (Aili et al., 2020)). The average temperature in the containments in service is estimated to be 25°C for F1 and F2 and 30°C for C1 and C2. For the Vercors mock-up, the actual temperature history is used. The relative humidity in service is estimated at 40% for the 4 containments and Vercors mock-up. Finally, the loading age depends on the containment considered.

Figures 10 to 17 compare the predicted vertical and tangential delayed deformations with those measured for the 4 containment, and figures 18 and 19 compare the predicted deformations with measurement for the Vercors mock-up. The comparison is also made with unadjusted regulatory laws (ξ_i values equal to 1). It can be seen that calibration on laboratory concrete tests allows for better prediction of delayed deformations and that, overall, delayed deformations are correctly predicted.

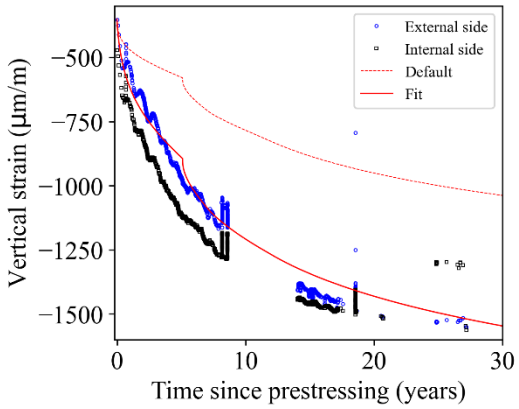

Figure 10: C1 Vertical strains

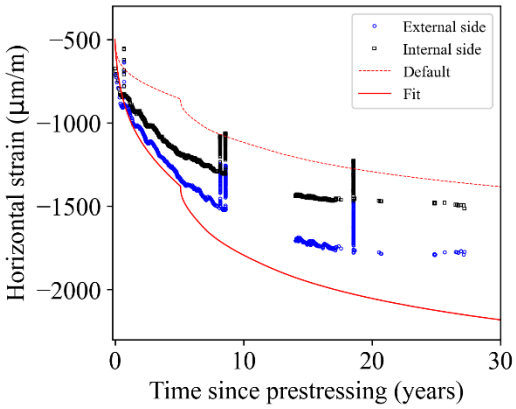

Figure 11: C1 Tangential strains

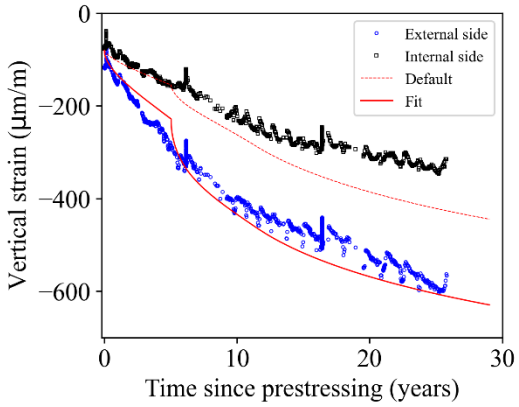

Figure 12: C2 Vertical strains

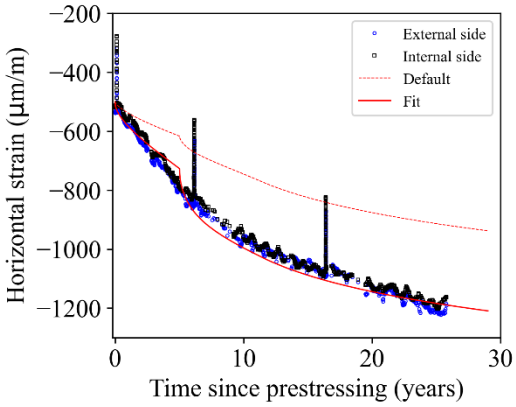

Figure 13: C2 Tangential strains

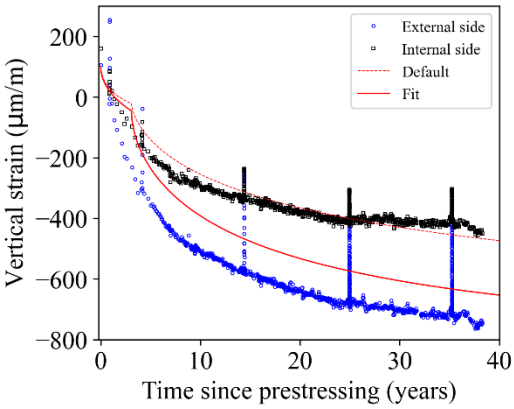

Figure 14: F1 Vertical strains

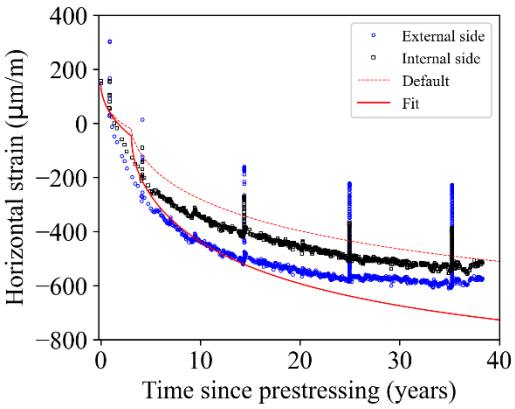

Figure 15: F1 Tangential strains

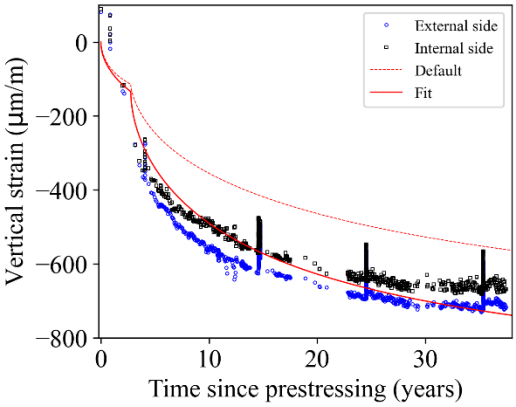

Figure 16: F2 Vertical strains

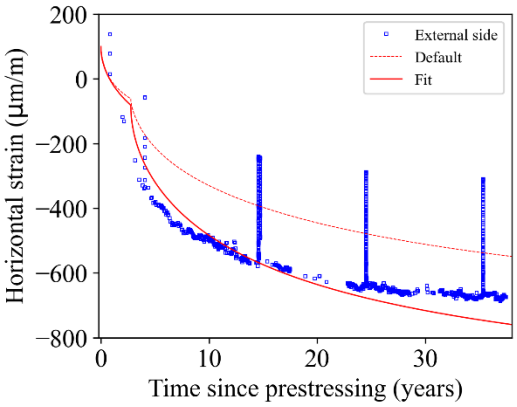

Figure 17: F2 Tangential strains

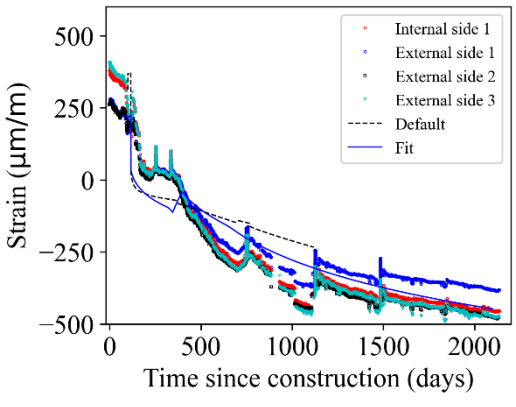

Figure 18: Vercors Vertical strains

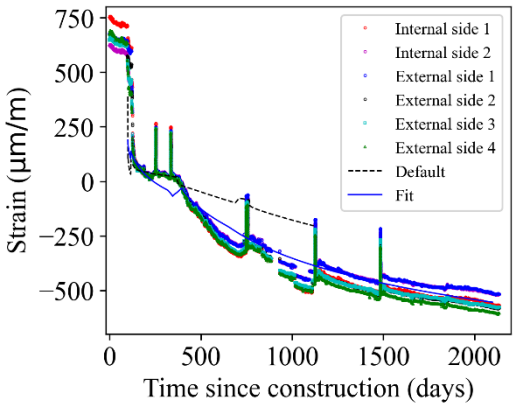

Figure 19: Vercors Tangential strains

5. Results analysis

For the total creep coefficient, the mean value over the seventeen containments is 1.27 times the theoretical value, the standard deviation is 0.38 and the coefficient of variation is 30 % (instead of 25 %, as indicated in MC2010). The theoretical value must be multiplied by 1.9 to obtain a safety factor for creep

with a fractile of 95 %.(this safety factor is the equal to $\mu + 1.645\ \sigma = 1.27 + 1.645 \times 0.38 = 1.89$, where μ is the mean value and σ is the standard deviation, and assuming a normal distribution).

For total shrinkage deformation, the mean value over the 17 containments is 1.02 times the theoretical value, the standard deviation is 0.39 and the coefficient of variation is 38 % (instead of 35 %, as indicated in MC2010). The theoretical value must be multiplied by 1.7 to obtain a safety factor for the drying shrinkage deformation with a fractile of 95 %. (this safety factor is equal to $\mu + 1.645\ \sigma = 1.02 + 1.645 \times 0.39 = 1.67$, where μ is the mean value and σ is the standard deviation, and assuming a normal distribution).

These results are consistent with the calibrations performed on laboratory tests (Table 2). However, in the future, the concrete specifications will include requirements on Young's modulus of the containment concrete (need to have a value greater than or equal to that given by the modulus-strength relationship) that did not exist before or, even better, specifications on the amplitudes of creep and shrinkage. It will allow a reduction of delayed deformations and, therefore, reduce the safety factor of the containment delayed deformations compared to that obtained on the old containments in service.

6. Conclusions

Delayed deformations of containment structures can be correctly predicted, provided shrinkage and creep laws are calibrated first on laboratory tests and then on the actual containment deformations. Indeed, given the natural variability of concretes, delayed deformations are predicted using the default laws and parameters of Eurocode 2 with significant uncertainty.

To hedge against this uncertainty because of the high stakes for nuclear containments, safety factors should be applied to shrinkage and creep if no information is available on the concrete used apart from its strength. Requirements on the concrete modulus or delayed deformations can reduce these coefficients. In any case, the parameters of the laws will be determined by laboratory tests.

Acknowledgment

The first, third, and fourth authors thank EDF for supporting this study.

Data availability

The data supporting this study's findings are available from the corresponding author, [JMT], upon reasonable request.

References

Abrishami, H., Tcherner, J., Barre, F., Borgerhoff, M., Bumann, U., Calonius, K., ... & Varpasuo, P. (2015). Bonded or unbonded technologies for nuclear reactor prestressed concrete containments (No. NEA-CSNI-R--2015-5). Organisation for Economic Co-Operation and Development.

AFNOR - 2005 - NF EN 1992-2 - Eurocode 2 - Design of concrete structures - Part 2: Concrete bridges — Design and detailing rules (2005)

AFNOR - 2007 – NF EN1992-1-1 NA – Eurocode 2 : Calcul des structures en béton — Partie 1-1 : Règles générales et règles pour les bâtiments - Annexe Nationale à la NF EN 1992-1-1 : (2005)

A. Aili, J.M. Torrenti, Modeling Long-term Delayed Strains of Prestressed Concrete with Real Temperature and Relative Humidity History, *Journal of Advanced Concrete Technology* Vol. 18, 396-408, July 2020

Aili, A., Torrenti, J. M., Sellin, J. P., Barthelemy, J. F., & Vandamme, M. (2023). On the long-term delayed strain of concrete structures. *Cement and Concrete Research*, 165, 107086.

A. Aili, J.M. Torrenti, F. Barré, L. Caba, Delayed deformation of confinement buildings: 30-Year in situ measured data and prediction with the next-generation Eurocode-2, Structural Concrete, 2024, https://doi.org/10.1002/suco.202300665

Anderson, P. (2005). Thirty years of measured prestress at Swedish nuclear reactor containments. *Nuclear engineering and design*, 235(21), 2323-2336.

Bažant, Z. P., Hubler, M. H., & Yu, Q. (2011). Excessive creep deflections: An awakening. *Concrete international*, 33(8), 44-46.

Bažant, Z. P., Yu, Q., & Li, G. H. (2012). Excessive long-time deflections of prestressed box girders. I: Record-

span bridge in Palau and other paradigms. *Journal of structural engineering*, 138(6), 676-686.
Bažant, Z. P., Yu, Q., & Li, G. H. (2012). Excessive long-time deflections of prestressed box girders. II: Numerical analysis and lessons learned. *Journal of Structural Engineering*, 138(6), 687-696.
Bouhjiti, D. M., Boucher, M., Briffaut, M., Dufour, F., Baroth, J., & Masson, B. (2018). Accounting for realistic Thermo-Hydro-Mechanical boundary conditions whilst modeling the ageing of concrete in nuclear containment buildings: Model validation and sensitivity analysis. Engineering Structures, 166, 314-338.
CEN, FprEN 1992-1-1:2022, Eurocode 2: Design of concrete structures - Part 1-1: General rules - Rules for buildings, bridges and civil engineering structures (2022)
L. Charpin, Julien Niepceron, Manuel Corbin, Benoît Masson, Jean-Philippe Mathieu, Jessica Haelewyn, François Hamon, Magnus Åhs, Sofía Aparicio, Mehdi Asali, Bruno Capra, Miguel Azenha, David E.-M. Bouhjiti, Kim Calonius, Meng Chu, Nico Herrman, Xu Huang, Sergio Jiménez, Jacky Mazars, Mahsa Mosayan, Georges Nahas, Jan Stepan, Thibaud Thenint, Jean-Michel Torrenti, Ageing and air leakage assessment of a nuclear reactor containment mock-up: VERCORS 2nd benchmark, Nuclear Engineering and Design 377 (2021), https://doi.org/10.1016/j.nucengdes.2021.111136
J.L. Costaz, J. Picaut, F. Barre – Evolution of the concrete containment in the French PWR program - SMIRT 7th – August 1983 - (http://www.lib.ncsu.edu/resolver/1840.20/26056)
J.L. Costaz, H. Rousselle, J. Picaut, J. Chataigner – Delayed Analysis from French PWR 900 MW containment Monitoring comparison with foreseen design values SMIRT 10 – August 1989
fib, ***fib*** Bulletin 65: Model Code 2010 Vol. 1, 2012.
L. Granger, Comportement différé du béton dans les enceintes de centrales nucléaires : analyse et modélisation (Ph.D. thesis), Ecole Nationale des Ponts et Chaussées (1995)
Hora, Z., & Patzák, B. (2007). Analysis of long-term behaviour of nuclear reactor containment. Nuclear engineering and design, 237(3), 253-259.
Lundqvist, P., & Nilsson, L. O. (2011). Evaluation of prestress losses in nuclear reactor containments. Nuclear engineering and design, 241(1), 168-176.
H.S. Müller, I. Anders, R. Breiner, M. Vogel, Concrete: treatment of types and properties in ***fib*** Model Code 2010, ***Struct****ural* ***Concre****te* 14 (2013) 320–334.
Shurbert-Hetzel, C., Daneshvar, D., Robisson, A., & Shafei, B. (2023). Data-enabled comparison of six prediction models for concrete shrinkage and creep. Case Studies in Construction Materials, 19, e02406**.**
Simon, A., & Courtois, A. (2011). Structural monitoring of prestressed concrete containments of nuclear power plants for ageing management. Structural Mechanics in Reactor Technology, 21, 6-11.
Šmilauer, V., Dohnalová, L., Jirásek, M., Sanahuja, J., Seetharam, S., & Babaei, S. (2023). Benchmarking Standard and Micromechanical Models for Creep and Shrinkage of Concrete Relevant for Nuclear Power Plants. Materials, 16(20), 6751.
Song, H. W., Kim, S. H., Byun, K. J., & Song, Y. C. (2002). Creep prediction of concrete for reactor containment structures. Nuclear Engineering and Design, 217(3), 225-236
Wendner, R., Hubler, M. H., & Bažant, Z. P. (2015). Optimization method, choice of form and uncertainty quantification of Model B4 using laboratory and multi-decade bridge databases. ***Materials and Structures***, 48, 771-796.